

Analytical Modeling of FRP-Reinforced Shear Walls Including Intermediate Crack Debonding Mechanisms



C.A. Cruz-Noguez, D.T. Lau & E. Sherwood

Department of Civil and Environmental Engineering, Carleton University, Ottawa

SUMMARY:

In reinforced-concrete (RC) shear walls repaired/strengthened with fiber-reinforced polymer (FRP) tow sheets, debonding of FRP material from the concrete substrate often controls the failure mode and overall response. A common debonding mechanism is that caused by the opening up of flexural cracks, also known as intermediate crack (IC) debonding. This paper presents an analytical model to predict the nonlinear response of RC shear walls repaired and strengthened in flexure with externally-bonded FRP sheets, implementing a computationally-simple procedure to account for IC debonding. The model is validated using experimental results. It is found that neglecting the influence of IC debonding produces significant overestimations of the load carrying capacity of the walls and an overall poor correlation between the analytical and experimental nonlinear response. In contrast, considering the effects of IC debonding leads to close agreement between calculated and measured ultimate strength, nonlinear hysteretic response and failure modes.

Keywords: cracking; debonding; FRP; model; shear wall

1. INTRODUCTION

Reinforced-concrete (RC) shear walls are a common type of lateral load resisting system found in structures located in seismically active regions. An attractive approach for repair and strengthening of shear walls in existing RC structures is the use of fibre-reinforced polymers (FRP) tow sheets due to the ease of installation, the high strength-to-weight ratio, and the high resistance to corrosion of FRP (Meier et al. 1992). Recently, experimental studies have been conducted to investigate the response of shear walls reinforced with FRP to enhance their flexural strength (Lombard et al. 2000; Hiotakis, 2004; Cruz-Noguez et al. 2012). Developing an accurate numerical model to predict the nonlinear response of a flexurally FRP-reinforced wall is crucial because of the possibility that the retrofit enhancement could lead to a failure mechanism controlled by shear instead of flexure. In addition, any valid numerical model of a FRP-reinforced structure must account for the eventual debonding between the FRP and the concrete substrate caused by flexural cracks in the concrete and how this mechanism affects the load carrying capacity and the hysteretic behaviour of the structure. While the analytical modeling of RC beams and slabs repaired/strengthened in flexure with FRP has been widely investigated (Teng et al. 2002; Wong and Vecchio, 2003; Oehler et al. 2003; Lu et al. 2007), there is still scant information on analytical modeling of shear walls with flexural FRP reinforcement (Khomwan 2010). This paper presents a numerical study on the simulation of the nonlinear response behaviour of seven shear wall specimens flexurally-reinforced with carbon FRP (CFRP) tow sheets and tested to failure in previous experimental studies at Carleton University (Lombard et al. 2000; Hiotakis 2004). The novel aspect of this investigation is the implementation of a simple procedure to simulate the debonding mechanism between the concrete substrate and the FRP material, based on the intermediate crack (IC) debonding research carried out by Lu et al. (2007). Consideration of this debonding process has not been taken into account in previous analytical studies of FRP-reinforced shear walls. The analytical results are compared with experimental data and good correlation is observed for key structural response parameters, such as initial stiffness, ultimate flexural capacity and failure mechanisms. The consideration of the IC debonding mechanism in the analytical model is

found to be crucial for a realistic and accurate simulation of the nonlinear response behaviour of the shear walls reinforced with FRP tow sheets.

2. INTERMEDIATE CRACK DEBONDING

2.1. Background

Debonding of FRP material from the concrete substrate often controls the failure mode and overall response of RC elements repaired/strengthened with FRP. If debonding is prevented from occurring, failure is typically associated with either compressive concrete crushing or FRP tensile rupture. Lu et al. (2007) reviewed the results of experimental tests on 77 beams and slabs strengthened with FRP and concluded that one of the most critical debonding mechanisms observed in those tests was that caused by the opening up of flexural cracks in the concrete. This debonding mechanism is referred as intermediate crack (IC) debonding (Teng et al. 2002).

2.2. Modeling of FRP-concrete debonding

Since IC debonding occurs at the location of major flexural cracks, proper modeling of the cracking process in the concrete is essential. Two different approaches have been developed using the finite-element method (FEM) to model concrete cracking: the discrete and the smeared crack models. In the discrete crack approach (Yang et al. 2003; Niu and Wu, 2006), the propagation of predefined, dominant cracks is captured by remeshing the model at each load step. In the smeared crack approach (Wong and Vecchio, 2003; Pham and Al-Mahaidi, 2007), an infinite number of parallel cracks are considered to be evenly distributed (“smeared”) over the element, and crack propagation is simulated by reducing the stiffness and strength of the concrete. Due to its simplicity compared with the more computationally-demanding discrete crack approach, the smeared crack approach was adopted in this study. For commonly used FRP-concrete adhesives, debonding is the result of a tensile fracture in a very thin (a few millimetres thick) concrete layer directly underneath the FRP laminate (Teng et al. 2002). Therefore, FE analyses with a very fine mesh are required to rigorously capture the development and propagation of the cracks that initiate the IC debonding mechanism. Such analyses are referred as meso-scale FE methods, in which the typical size of the elements is one order smaller than the assumed thickness of concrete that experiences tensile fracture at debonding (common element sizes are of the order of 0.5 mm). In the meso-scale method, the elements representing the FRP laminate are connected to those representing the concrete using the “common node” method, and the adhesive layer between the FRP and the concrete is not explicitly modeled. This is because it is assumed that the amount of interfacial slip occurring at the adhesive layer is negligible compared to the amount of slip experienced by the concrete layer adjacent to the adhesive (Lu et al. 2005). Excellent correspondence between measured and calculated results (in terms of load-deflection curves, crack patterns and debonding progression) was reported by Lu et al. (2007) using the meso-scale method to simulate the response of two FRP-strengthened beams tested by Wu and Yin (2003). Although accurate and amenable for implementation in most FE packages, the meso-scale method is not suitable to study common-size structures due to the high computation cost resulting from the small FE mesh size used. As an alternative, the use of FRP-concrete interface elements with bond-slip constitutive laws that simulate the mechanics of the debonding caused by the tensile fracture in the concrete layer has been proposed (Wong and Vecchio, 2003; Wu and Yin, 2003; Ebead and Neale, 2007; Lu et al. 2007). Since the interface elements already account for the FRP-concrete interaction, this alleviates the need of a fine FE mesh as required for a conventional meso-scale analysis. Typically, bond-slip relationships obtained from experimental FRP-concrete pull tests are used to define the constitutive laws of these interface elements (Ebead and Neale, 2007). Since usual FRP-concrete pull tests are conducted using uncracked concrete prisms, a serious limitation in this approach is that these models can not capture the potential influence that debonding caused by opening of flexural cracks (IC debonding) has on the overall behaviour of common structural members subjected to flexure (Sato, 2003). To overcome this limitation, Lu et al. (2007) obtained representative bond-slip relationships for FRP-concrete interfaces with and without major flexural cracks using meso-scale

finite-element simulations. For FRP-concrete interfaces outside major flexural crack zones, the bond-slip model developed by Lu et al. (2005), referred as Bond-Slip Model I and derived from usual FRP-uncracked concrete pull tests agrees closely with the results obtained using the meso-scale method (Fig. 2.1). For the interface behaviour inside the flexural crack zone, Lu et al. (2007) modified Bond-Slip Model I to account for the brittle response of the FRP-concrete bond-slip relationship predicted by the meso-scale method (notice the significant drop in average bond stresses at crack zones of width equal to 15 and 20 mm in Fig. 2.1 for slips equal to s_0). The resulting model was referred as Bond-Slip Model II. Bond-Slip Models I and II were adopted in this study to account for the influence of flexural cracks on the bond-slip interaction between the FRP material and the concrete substrate. Note that Bond-Slip Models I and II are identical up to slips equal to s_0 , the interfacial slip associated to the maximum shear bond stress τ_{max} , and the only difference between the models is the post-peak brittle behaviour in Bond-Slip Model II.

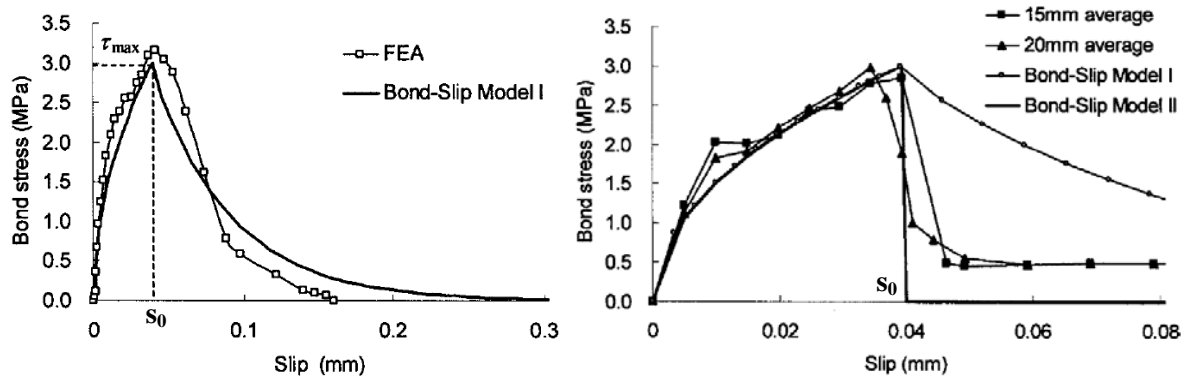


Figure 2.1. Bond-slip curves for FRP-concrete zones outside (left) and inside (right) major flexural crack zones (Lu et al. 2007)

3. MODELING OF FRP-REINFORCED WALLS

The FE program VecTor2 (Wong and Vecchio, 2002) was used to analyze the cyclic response of the tested walls. Program VecTor2 allows for the modelling of concrete under normal and shear stresses as an orthotropic material with smeared, rotating cracks. Four-node quadrilateral elements are used to model the concrete (Fig. 4.1). The foundation was not included in the model since it was assumed to be very rigid compared to the wall. To model the concrete pre-peak and post-peak response behaviour, the Popovics and the modified Park-Kent model were used, respectively. To model the steel rebars and stirrups, the various reinforcement ratios at different regions of the wall were modeled as uniformly-distributed reinforcement. The steel rebar material was modelled as an elastic-plastic material with strain hardening.

The CFRP sheets were modelled with a series of discrete truss elements made of a brittle material with zero compressive strength. The connection between the CFRP truss elements and the concrete at the bottom of the wall is represented using the common-node method since mechanical anchorage between FRP and concrete is provided at the base. For the rest of the wall, zero-length link elements were used to connect the FRP trusses and the concrete elements. The bond-slip relationship selected for the link elements is that given by a tri-linear approximation to Bond-Slip Model I (Lu et al. 2005), calculated based on the material properties of the concrete, as shown in Fig. 4.1. The interface elements follow Bond-Slip Model I if the concrete does not have major flexural cracks, and Bond-Slip Model II if major flexural cracks are present. A “major flexural crack” is defined here as a crack that produces a total slip in the FRP-concrete interface greater than s_0 . Thus, careful monitoring of the crack widths in all concrete elements during each load step is required. It is assumed that if a flexural crack of width w appears in a concrete element, the interfacial FRP-concrete slip, s , that occurs at both sides of the flexural crack are equal to $w/2$. Since IC debonding is considered to take place if $s > s_0$ (Bond-Slip Model II applies and the bond strength becomes zero), the crack width in a concrete

element that causes FRP-concrete debonding should be therefore greater or equal to $2s_0$. Conversely, if w is less than $2s_0$, Bond-Slip Model I (derived from pull tests with no flexural cracks in the concrete prism) applies and the two materials remain bonded. A mesh of regular size (with element length sizes varying from 30 to 45mm) was used to discretize the wall. Note that meso-scale techniques would have required element sizes approximately 80-100 times smaller to rigorously account for IC debonding. Instead, the use of FRP-concrete interface elements in this study (with bond-stress relationships that are different for cracked and uncracked concrete) allows for the use of regular mesh sizes and thus a more computationally-efficient model. The implementation of the debonding subroutine was conducted with a simple, three-step procedure, described as follows:

At the end of each load step (step i):

1. Store seed file (file recording the stressed state of all elements in the model) generated at the end of load step i .
2. Monitor results of load step i for any concrete element where the crack width is greater or equal than $2s_0$. For each of such elements, modify the FE model deactivating all link elements adjacent to that concrete element.
3. Continue the analysis using the modified FE model for load step $i + 1$ using the seed file obtained at the end of load step i .

Note that for the seed file of step i to be valid as a starting point of step $i + 1$, a sufficiently small load/displacement increment needs to be used during the analysis, so any deactivated link element do not produce significant changes to the stiffness matrix of the structure. In this study, load displacements of 1 mm and 5 kN were used with satisfactory results.

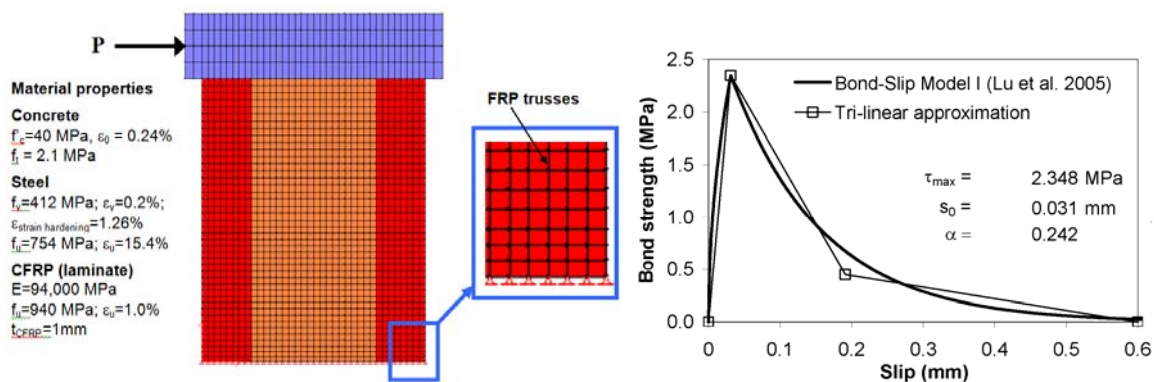


Figure 4.1. Generic FE shear wall model (left) and tri-linear bond-slip relationship for interface elements (right)

4. SHEAR WALL EXPERIMENTAL TESTS

The effectiveness of CFRP reinforcement oriented in the vertical direction to repair and strengthen RC shear walls for flexure enhancement has been investigated by Lombard et al. (2000) and Hiotakis (2004) in a comprehensive test program of nine cantilevered 1.8x1.5x0.1 m shear wall specimens (Fig. 2.1). The CFRP repair/strengthening scheme is shown in Table 2.1. Details of the specimens and test results are discussed by Cruz-Noguez et al. (2012). Fig. 4.2 presents the envelopes of the hysteretic relationships between the base shear and top deflection of the wall specimens measured during the experiments. In general, it is observed that all repaired and strengthened walls exhibit a significantly larger maximum load carrying capacity (up to 197% in the case of SW3-2) and higher ductility (up to 194% in RW1) compared to the CW specimens. The first sign of damage in the test specimens is cracking of the concrete near the base, starting in areas adjacent to the two sides of the wall. Debonding of the CFRP sheets from the concrete substrate typically follows. In repaired walls, debonding of the CFRP sheets started at zones of the wall where pre-existing cracks re-opened. In strengthened specimens, debonding of the FRP sheets was observed first at the edges of the wall, at zones where there are major flexural cracks. In both repaired and strengthened walls, debonding of the FRP sheets starts at the edges of the wall, near the plastic hinge region. After a few reversed loading

cycles, debonding of the FRP sheets propagated rapidly first towards the center of the wall and then upwards. This separation between FRP and the concrete substrate has a major impact on the nonlinear response of the walls, as discussed by Cruz-Noguez et al. (2012).

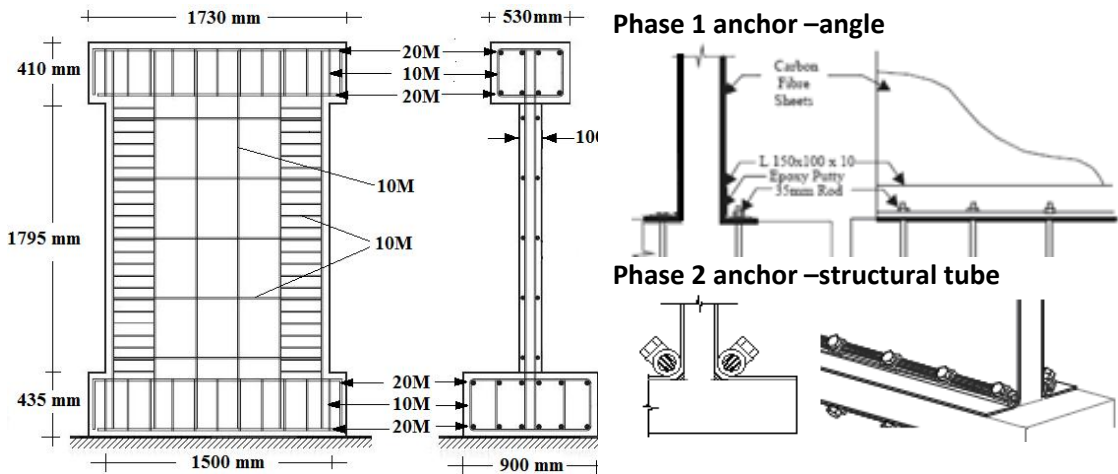


Figure 4.1. Shear wall and anchor system details

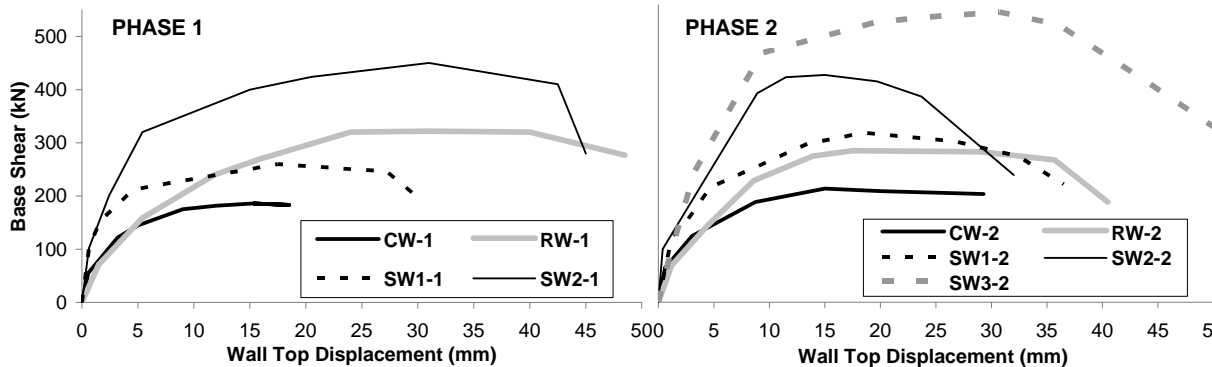


Figure 4.2. Force-displacement envelopes

Table 1.1. Repair/Strengthening Schemes (Lombard et al. 1999; Hiotakis, 2004)

Phase	Anchor type	Type of Specimen	Repair/Strengthening Scheme*	Code
1	Angle	Control	---	CW-1
		Repaired	1V	RW-1
		Strengthened	1V	SW1-1
		Strengthened	2V + 1H	SW2-1
2	Tube	Control	---	CW-2
		Repaired	1V	RW-2
		Strengthened	1V	SW1-2
		Strengthened	2V	SW2-2
		Strengthened	3V + 1H	SW3-2

*: nV = Wall reinforced with n layers of unidirectional FRP on each side in the vertical direction
 *: mH = Wall reinforced with m layers of unidirectional FRP on each side in the horizontal direction

5. FINITE-ELEMENT RESULTS AND DISCUSSION

5.1. Plain RC walls

To evaluate the ability of the FE program used in this study to model the behaviour of plain RC shear walls, the calculated base shear – top displacement response of specimens CW-1 and CW-2 are compared with the measured results (Fig. 5.1). Note that walls CW-1 and CW-2 had no FRP

reinforcement because they were intended to serve as a reference for the behaviour of conventional RC walls subjected by moderate to large earthquakes. It is observed that the experimental response in terms of strength, initial stiffness and energy dissipation are closely predicted by the analytical model.

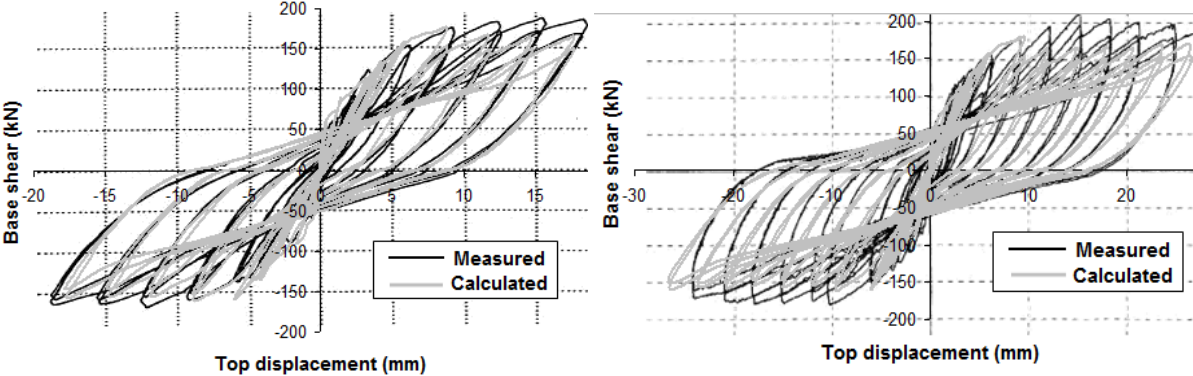


Fig. 5.1 Calculated vs. measured response of plain RC walls

5.2. FRP-Strengthened walls

Before discussing simulation results with IC debonding effects included, it is convenient to review the wall response that would be determined using typical FE analyses of FRP-reinforced structures, this is, neglecting IC debonding effects and using with interface elements with bond-slip laws derived only from typical FRP-concrete pull tests. Due to space limitations, only results for specimen SW1-1 are shown in Fig. 5.2 (results for all other walls are found to be similar). It is seen that neglecting the effects of the IC debonding leads to significant overestimation of the maximum load carrying capacity of the wall and an overall poor correlation between the calculated and measured hysteretic response. With IC debonding being neglected, the FRP remains bonded to the concrete and carrying load for crack widths larger than $2s_0$, with the bond stress at the FRP-concrete link elements being given by the parabolic bond-slip relationship in Fig. 4.1. As long as the bond stress is greater than zero, stresses continue being transferred from the concrete elements to the FRP truss elements. Eventually, the stresses at the FRP reach the tensile strength of the material and the FRP fractures in a brittle manner (notice the sudden drop in load carrying capacity at a top displacement of -19 mm in Fig. 5.1). In contrast, when considering IC debonding effects, the FRP is separated from the concrete as soon as FRP-concrete slips exceed s_0 , which translates into a more gradual loss of load carrying capacity since FRP-concrete separation occurs before the FRP trusses fracture. This agrees with the experimental observations on the behavior of walls reinforced with flexural FRP tow sheets (Lombard et al. 2000; Hiotakis 2004) where FRP-concrete debonding, first occurring at zones of the wall with the largest tensile stresses (wall edges at the bottom part of the specimen), generally preceded FRP tearing at those locations. An additional observation can be made in regards to the prediction of initial stiffness: since debonding does not usually occur at low displacement levels, the prediction of initial stiffness is similar for both types of analysis, as shown in Fig. 5.2.

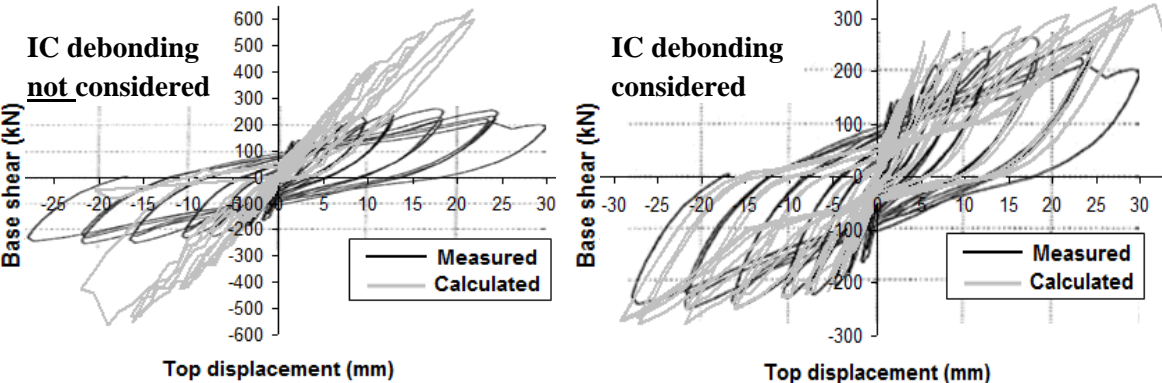


Fig. 5.2 Influence of IC debonding mechanism on the response of specimen SW1-1

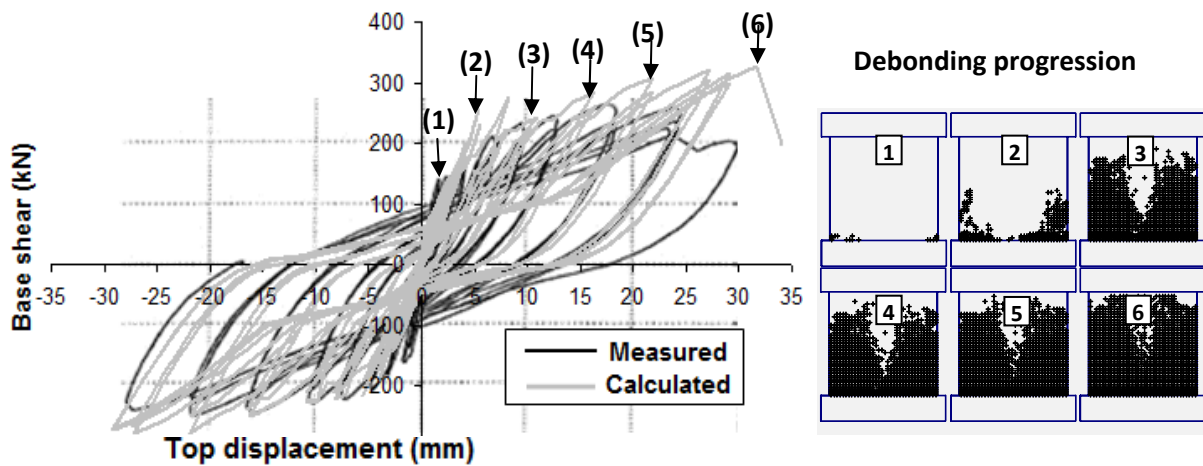


Fig. 5.3 Detailed debonding progression in specimen SW1-1

The calculated responses of specimens SW1-2, SW2-1, SW2-2 and SW3-2 are shown in Fig. 5.4. Overall, it is seen that the model leads to a reasonable correlation between analytical and experimental results in all specimens.

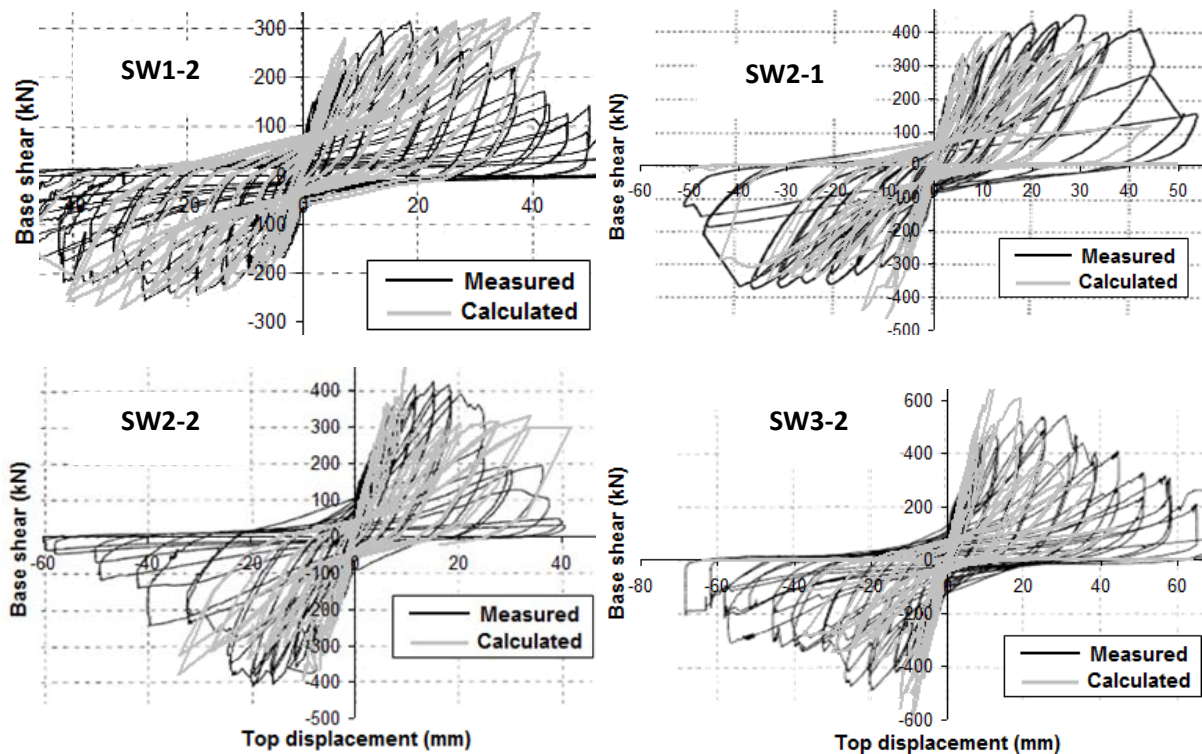


Fig. 5.4 Calculated vs. measured response of SW specimens (IC debonding considered)

To compare the observed debonding status of the walls with the model predictions, two walls were analyzed. The observed and predicted debonding for strengthened walls with a single layer of FRP (SW1-1 and SW1-2) were compared at the displacement associated to their corresponding maximum load strength (Fig. 5.5). It is seen that there is a reasonable correspondence between calculated and measured results. IC debonding is more pronounced at the edges of the wall, and less significant at the central zone, where bending stresses (and thus concrete cracking) are not as significant as those

occurring at the wall edges.

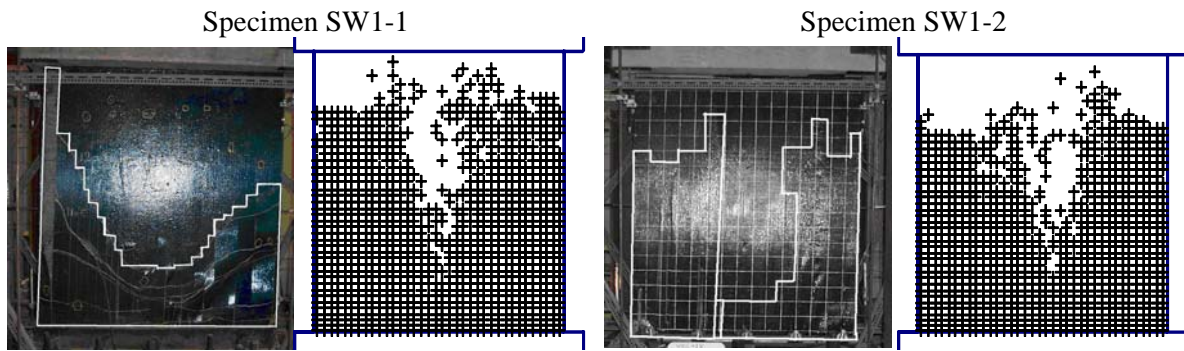


Fig. 5.5 Observed and predicted debonding in SW specimens

5.3. FRP-Repaired walls

The RW specimens were modeled by using two separate, superimposed mesh layers of concrete elements and one layer of FRP trusses. The repair procedure was simulated using two steps. In the first step, only one layer of concrete elements is active, while the layer of FRP trusses is inactive. The stiffness of the elements of an “active” layer is added to the stiffness matrix of the structure, while the stiffness of those in an “inactive” layer is not. The walls were then analyzed as CW-1 and CW-2. In the second step, the active (now cracked) mesh of concrete elements at the bottom half of the wall is deactivated, while the previously inactive (and undamaged) layer of concrete elements is activated to simulate repair to the damaged concrete material (filling of the cracks with mortar). The FRP trusses are activated in this step to simulate the application of CFRP tow sheets after the cracks have been filled. The walls are then re-analyzed as RW-1 and RW-2. The calculated force-displacement responses of both walls are shown in Fig. 5.6. It is observed that although the overall correlation between the calculated and measured response is limited, the predictions of initial stiffness and maximum strength are reasonable.

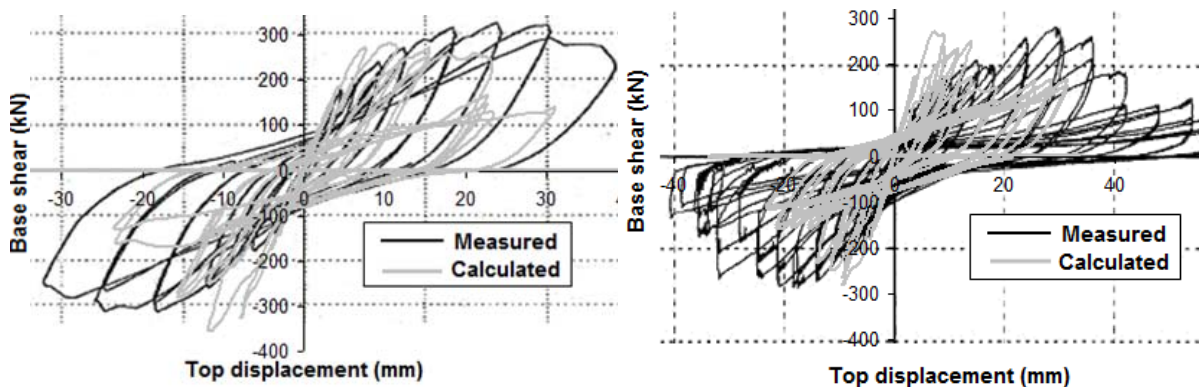


Fig. 5.6 Calculated vs. measured response of RW specimens (IC debonding considered)

6. CONCLUSIONS

This paper presented the analytical modeling of walls repaired and strengthened using externally-bonded CFRP reinforcement in flexure. The conclusions that can be drawn from the study are the following:

- a) The intermediate crack (IC) debonding mechanism has been shown to be an important factor that controls the behaviour of FRP-reinforced walls in terms of maximum load capacity and nonlinear hysteretic response. IC debonding does not have a significant effect on the prediction of initial stiffness.

- b) The modeling process presented in this paper has been shown to be effective in predicting satisfactorily the response of strengthened walls with a single layer of FRP per side in terms of initial stiffness, maximum load capacity and nonlinear hysteretic behaviour. The model gives reasonable correlation between calculated and measured results for strengthened walls with more than one FRP layer per side.
- c) In repair applications, the analytical model has been shown to be capable to accurately predict the initial stiffness and produce reasonable estimates of maximum load capacity, but the prediction of the nonlinear response may still need some improvement.
- d) The debonding criterion used in this study is simple and easy to implement into FE packages that do not allow the development of user-defined elements, such as the one used in this study.

ACKNOWLEDGEMENT

Financial support provided by Public Works and Government Services Canada (PWGSC) for the experimental part of the program is acknowledged. The technical assistance provided by Dr. Simon Foo of PWGSC for the experimental tests is appreciated. The authors gratefully acknowledge the funding provided for the analytical portion of this study by the Canadian Seismic Research Network (CSRN) under the National Sciences Engineering Research Council (NSERC) strategic national grant program.

REFERENCES

- Antoniades, K., Salonikios, T., and Kappos, A. (2003). Cyclic Tests on Seismically Damaged Reinforced Concrete Walls Strengthened Using Fiber-Reinforced Polymer Reinforcement. *ACI Struct. J.* **100:4**, 510-518.
- Cruz-Noguez, C., Lau, D. T., Sherwood, E., Lombard, J., and Hiotakis, S. (2012). Repair and strengthening of RC shear walls using externally-bonded FRP sheets. *6th International Conference on Advanced Composite Materials in Bridges and Structures (ACMBS-VI)*. Accepted for publication.
- Hiotakis, S. (2004). Repair and Strengthening of Reinforced Concrete Shear Walls for Earthquake Resistance Using Externally Bonded Carbon Fibre Sheets and a Novel Anchor System. Master's thesis, Department of Civil and Environmental Engineering, Carleton University.
- Khalil, A. and Ghojarah, A. (2005). Behaviour of Rehabilitated Structural Walls. *J. of Earthquake Eng.*, **9:3**, 371-391.
- Khomwan, N., Foster, S. J., Smith, S. T. (2010). FE modeling of FRP-repaired planar concrete elements subjected to monotonic and cyclic loading. *ASCE J. of Comp. for Constr.*, **14:6**, 720-729.
- Lombard, J., Lau, D., Humar, J., Foo, S. and Cheung, M. (2000). Seismic strengthening and repair of reinforced concrete shear walls. *12th World Conf. on Earthquake Eng.*, Paper No. 2032.
- Lu, X. Z., Teng, J. G., Ye, L. P., and Jiang, J. J. (2005). Meso-scale finite-element model for FRP sheets/plates externally bonded to concrete. *Eng. Struct.*, **27:6**, 564-575.
- Lu, X. Z., Teng, J. G., Ye, L. P., and Jiang, J. J. (2007). Intermediate crack debonding in FRP-strengthened RC beams: FE analysis and strength model. *ASCE J. of Comp. for Constr.*, **11:2**, 161-174.
- Meier, U., Dearing, M., Meier, H, and Schwengler, G. (1992). Strengthening of Structures with CFRP Laminates: Research and Applications in Switzerland. *1st Int. Conf. on Adv. Comp. Mater. in Bridges and Struct.*, **Vol. 1:243-251**.
- Oehler, D.J., Park, S.M. and Mohamed Ali, M.S. (2003). A structural engineering approach to adhesive bonding longitudinal plates to RC beams and slabs. *Composites, Part A.* **34:12**, 887-897.
- Pham, H. and Al-Mahaidi, R. (2007). Modelling of CFRP-concrete shear-lap tests. *Int. J. of Constr. and Bldg. Mater.*, **21**, 727-735.
- Sato, Y. (2003). Mechanical characteristics of retrofitted members. *Technical Rep. of the JCI Technical Committee on Retrofit Technology*, 62-78.
- Teng, J. G., Chen, J. F., Smith, S. T., and Lam, L. (2002). FRP-strengthened RC structures, Wiley, London.
- Wong, S. Y., and Vecchio, F. J. (2003). Towards modeling of reinforced concrete members with externally bonded fiber-reinforced polymer composites. *ACI Struct. J.* **100:1**, 47-55.